Effects of geometrical shape dispersion on inhomogeneous broadening of excitonic peaks of semiconductor nano-objects

L. M. Thu,* W. T. Chiu, and O. Voskoboynikov

Department of Electronic Engineering and Institute of Electronics, National Chiao Tung University, Hsinchu 300, Taiwan

(Received 17 September 2010; revised manuscript received 29 January 2011; published 14 March 2011)

We present an efficient method for simulation of the inhomogeneous broadening of photoluminescence peaks of dispersive ensembles of semiconductor nano-objects. Using our mapping method for geometrical and material parameters of the objects, we managed to connect the position, asymmetry, and width of the photoluminescence emission peaks of ensembles of the objects to the actual dispersion of the geometrical shapes of the objects. The mapping method allows us to very efficiently reproduce and explain experimental data on the photoluminescence of dispersive ensembles of triple concentric GaAs/AlGaAs nano-rings, i.e., nano-objects with a very sophisticated three-dimensional geometry.

DOI: 10.1103/PhysRevB.83.125301 PACS number(s): 73.21.La, 78.67.Hc, 78.20.Bh

I. INTRODUCTION

Advances in modern semiconductor technologies make it possible to produce and investigate in detail semiconductor nano-objects (quantum dots, quantum dot molecules, nano-rings, etc.) within a wide range of geometrical shapes and material parameters. The nano-objects demonstrate very promising properties for practical use in modern optics, but the inherent dispersion of their geometrical parameters (shape and size) leads to the almost uncontrollable inhomogeneous broadening[1–4] in optical spectra. Simulations of the inhomogeneous broadening for ensembles of semiconductor quantum dots with simple spherical or cubic shapes are known in the literature (see, e.g., Refs. 2 and 3, and references therein). The broadening was explained as a result of the dot-size (volume) primitive dispersion. In addition, the excitonic effects and homogeneous broadening (which originated from the temperature fluctuations) have been ignored. Those approximations allow one to simulate the broadening using simple analytical expressions or nonextensive numerical simulations.

The optical characteristics of dispersive ensembles of semiconductor nano-objects of complex geometries and material compositions should be simulated using the multidimensional (multiparametric) distribution function, which cumulatively reproduces variations of the object parameters. Using the mapping method (recently derived by us),[5,6] we are able to very efficiently compute energy states and wave functions of electrons and holes confined in the nano-objects within a wide range of sizes, shapes, and compositions. Thus, we can simulate ensembles with multiparametric distributions. To demonstrate our method, in this paper we theoretically study the optical characteristics of triple concentric nano-rings, which possess much more sophisticated shape than quantum dots.

Semiconductor single nano-rings (see, e.g., Refs. 7 and 8, and references therein) attracted much attention at first because they are (unlike quantum dots) nonsimply connected nano-objects and the Aharonov-Bohm (AB) effect[9] in them offers an exclusive opportunity to monitor phases of the electronic wave functions. Some experimental evidence of the optical AB effect has been discovered in the photoluminescence spectra of InAs/GaAs nano-rings. Magneto-optical characteristics of single nano-rings were theoretically and experimentally investigated in detail (see Refs. 7–17, and references therein).

Very recently, using the droplet epitaxy technique, multiple concentric GaAs/Al $_x$Ga$_{1-x}$As nano-rings were fabricated with high material uniformity and excellent rotational symmetry.[18–20] The photoluminescence spectra of ensembles of triple concentric nano-rings were measured at low temperature ($T = 14$ K).[20] A wide asymmetrical emission peak near 1.56 eV was demonstrated with the full width at half maximum of 30 meV. The authors[20] provided some preliminary simulation results on the peak position and shape, but they did not explain why the peak is so wide and asymmetrical. We should stress that the wide asymmetrical peak certainly demonstrates the importance of the inhomogeneous broadening[1–4] in ensembles of the rings. Clearly, to predict and control the optical properties of dispersive ensembles of the rings, we have to possess complete understanding of the rings' geometrical and material dispersions.

In this paper, we perform a detailed simulation of the photoluminescence spectra of ensembles of the triple concentric nano-rings (see Fig. 1) and address the issue of the asymmetrical inhomogeneous broadening of the emission peaks. To reproduce actual geometrical and material parameters of the rings, we use our mapping method. Then we calculate energies of the excitonic optical transitions. We obtain the actual optical emission spectra in good agreement with the experiment by averaging the excitonic optical characteristics of the rings within their dispersive ensembles.

II. THEORY

To analyze dispersive ensembles of nano-objects of complex geometrical shapes, we should define a multidimensional (multiparametric) distribution function $P(\{x_i\})$ that describes dispersions of all appropriate parameters $\{x_i\}$ (such as size, anisotropy in geometry, composition, etc.). This function gives the number of the nano-objects in the ensemble dN with the values of $\{x_i\}$ inside the domain $\{x_i, x_i + dx_i\}$ as

$$dN = \prod_i P(\{x_i\})dx_i. \quad (1)$$

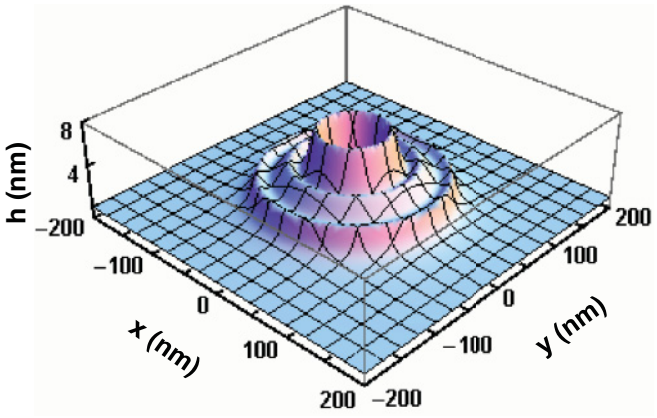

FIG. 1. (Color online) Three-dimensional geometrical shape of a triple concentric nano-ring.

In our consideration we assume that, in typical nano-object ensembles, the parameters follow the noncorrelated normal distribution, which is presented by

$$P(\{x_i\}) = P_G(x_1) \cdot P_G(x_2) \cdots, \tag{2}$$

where the standard normal distribution for each parameter x is written as

$$P_G(x) = AG\left(\frac{x - x^0}{\triangle x}\right), \tag{3}$$

and A is the normalization coefficient, x^0 is a mean value, $\triangle x$ is the standard deviation of the parameter x, and $G(y)$ is the Gaussian function. Now we can write the meaningful average for any physical quantity $Q(\{x_i\})$ characterizing the ensemble as

$$\bar{Q} = \int_{x_i} P(\{x_i\})Q(\{x_i\}) \prod_i dx_i. \tag{4}$$

Applying our approach in this study, we are able to describe the general broadening (combining the homogeneous and inhomogeneous broadenings) of excitonic peaks of ensembles of nano-objects. We start from the simulation of an individual nano-object, but at the same time we should be able to vary the object parameters. To satisfy this crucial requirement, we use our mapping method, which allows us to map realistic geometrical shapes, strains, and material compositions of semiconductor nano-objects (known from experiments) to smooth three-dimensional effective potentials for electrons and holes confined in the objects. We can consider semiconductor nano-objects within wide ranges of changes of radii, height, anisotropy in geometry, and composition. Then we are able to simulate the average intensity of excitonic optical transition by using the multidimensional distribution function $P(\{x_i\})$. To demonstrate the method, as an example, we consider a dispersive ensemble of triple concentric nano-rings with optical properties that are formed by a complex variation of the rings' shapes (Fig. 1). For these nano-objects, we choose the rings' local heights and radii to be our dispersive parameters x_i (Fig. 2).

In order to make this paper more self-contained, we briefly repeat some of the aspects of the mapping procedure presented in Ref. 5 (i.e., applying the mapping method specifically to the triple concentric nano-rings). We reproduce the actual

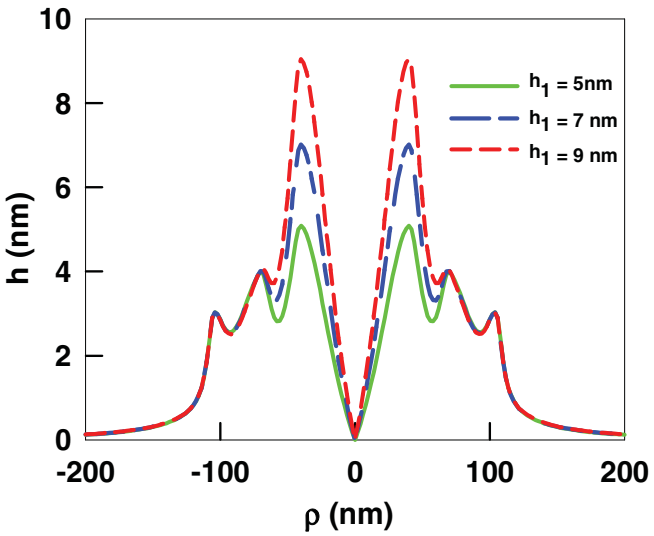

FIG. 2. (Color online) Two-dimensional geometry of triple concentric nano-rings with variation of the inner height $h_1(\rho = \sqrt{x^2 + y^2})$.

geometry of a triple concentric nano-ring by mapping the local heights of the ring according to experimental data reported in Ref. 20. The atomic force microscopy[20] shows that the triple concentric nano-rings are formed with good rotational symmetry (see Fig. 1) around the system growth direction (z axis). We accordingly assume that the triple concentric nano-rings are formed on a flat substrate parallel to the xy plane and we can model the ring shape by a function $h(x,y)$, which reproduces the local ring's height (along z direction) at the actual position on the xy plane (see Fig. 2). The function $h(x,y)$ can be presented by the following expression:

$$h(x,y) = \sum_{k=1}^{3} h_k(x,y),$$
$$h_k(x,y) = \begin{cases} h_{mk} \frac{\gamma_{ok}^2}{R_k^2} \frac{R_k^2 - (\sqrt{x^2+y^2} - R_k)^2}{(\sqrt{x^2+y^2} - R_k)^2 + \gamma_{ok}^2}, & \sqrt{x^2+y^2} \leqslant R_k, \\ h_{mk} \frac{\gamma_{ik}^2}{(\sqrt{x^2+y^2} - R_k)^2 + \gamma_{ik}^2}, & \sqrt{x^2+y^2} > R_k, \end{cases} \tag{5}$$

where R_k ($k = 1$, 2, and 3, respectively) is the radial position of the inner, middle, and outer rims, h_{mk} is the height of the kth rim, and γ_{ok} and γ_{ik} determine the inside and outside slopes of the kth rim. We present the three-dimensional smooth-confinement potential for electrons (holes) by the composition- and geometry-dependent profiles of the local conduction-band (e) and valence-band (h) edges,[5,6,21–23]

$$V_{e(h)}(\mathbf{r}) = \Delta E_{c(v)}(\mathbf{r}) = \Delta E_{c(v)}^0 \left\{1 - \frac{1}{4}\left[1 + \tanh\left(\frac{z}{a}\right)\right] \times \left[1 - \tanh\left(\frac{z - h(x,y)}{a}\right)\right]\right\}, \tag{6}$$

where $\mathbf{r} = (x,y,z)$ is the three-dimensional radius vector, $\Delta E_{c(v)}(\mathbf{r})$ is the local value of the conduction-band (valence-band) offset, $\Delta E_{c(v)}^0 = E_{c(v)}^{\text{out}} - E_{c(v)}^{\text{in}}$ is the overall band offset between the inner and outer semiconductor materials in their heterostructures,[5,6] and superscript "in" and "out" denote the actual material parameters inside and outside the rings. The

slope and range of the potential change at the boundaries of the ring are controlled by a parameter a. For instance, in the case of the hard-wall confinement ($a \to 0$), Eq. (6) provides $V_{e(h)}(\mathbf{r}) = 0$ (if $\mathbf{r}$ is inside the ring) and $V_{e(h)}(\mathbf{r}) = \Delta E^0_{c(v)}$ (if $\mathbf{r}$ is outside the ring).

Now we use $V_e(\mathbf{r})$ to define the mapping function,

$$M(\mathbf{r}) = 1 - \frac{V_e(\mathbf{r})}{\Delta E^0_c}. \tag{7}$$

This function accumulates experimental information about geometrical shapes and compositions of the rings and it allows us to present the position-dependent effective mass of electrons (holes), band gap, and dielectric constant of the system as the following:[5,6,22,23]

$$m_{e(h)}(\mathbf{r}) = m^{\text{in}}_{e(h)} M(\mathbf{r}) + m^{\text{out}}_{e(h)}[1 - M(\mathbf{r})], \tag{8}$$

$$E_g(\mathbf{r}) = E^{\text{in}}_g M(\mathbf{r}) + E^{\text{out}}_g[1 - M(\mathbf{r})], \tag{9}$$

$$\epsilon(\mathbf{r}) = \epsilon^{\text{in}} M(\mathbf{r}) + \epsilon^{\text{out}}[1 - M(\mathbf{r})]. \tag{10}$$

The electron (hole) wave functions $\Psi_{e(h)}(\mathbf{r})$ satisfy the following effective Schrödinger equation:

$$\hat{H}_{e(h)}(\mathbf{r})\Psi_{en(hm)}(\mathbf{r}) = E_{en(hm)}\Psi_{en(hm)}(\mathbf{r}), \tag{11}$$

where $\hat{H}_{e(h)}(\mathbf{r})$ is the one-band effective Hamiltonian for the electrons (holes),[21]

$$\hat{H}_{e(h)}(\mathbf{r}) = \frac{1}{2}\hat{\mathbf{p}}\frac{1}{m_{e(h)}(\mathbf{r})}\hat{\mathbf{p}} + V_{e(h)}(\mathbf{r}), \tag{12}$$

and $\hat{\mathbf{p}} = -i\hbar\nabla$ is the momentum operator and $n(m)$ are the electron (hole) quantum numbers.

For an exciton localized in the ring, using solutions of Eq. (11), we can estimate the excitonic binding energy in the ground state as[24]

$$E_c = -e\int d\mathbf{r}\Psi^*_{e0}(\mathbf{r})V_{h0}(\mathbf{r})\Psi_{e0}(\mathbf{r}), \tag{13}$$

where $V_{h0}(\mathbf{r})$ is a potential which satisfies the Poisson equation[25]

$$\epsilon_0\nabla_{\mathbf{r}}[\epsilon(\mathbf{r})\nabla_{\mathbf{r}}V_{h0}(\mathbf{r})] = -\rho_h(\mathbf{r}), \tag{14}$$

and $\rho_h(\mathbf{r})$ is the charge density of the hole in the ground state, $\rho_{h0}(\mathbf{r}) = e\Psi^*_{h0}(\mathbf{r})\Psi_{h0}(\mathbf{r})$.

The ground-state excitonic-transition energy now reads

$$E_{\text{ex}} = E_{e0} + E_{h0} + E^{\text{in}}_g + E_c, \tag{15}$$

where $E_{e(h)0}$ is the electron (hole) ground-state energy.

The intensity of the excitonic optical transitions, like a function of the transition energy E averaged within the ensemble of the rings, can be presented by the following expression:

$$\bar{I}(E) = \int_{x_i} P(\{x_i\})I(E,\{x_i\})\prod_i dx_i, \tag{16}$$

where for an individual ring with the certain set of parameters $\{x_i\}$, the excitonic peak is conventionally modeled by the normalized Lorentz distribution function

$$I(E,\{x_i\}) = \frac{1}{\pi}\frac{\Gamma}{[E - E_{\text{ex}}(\{x_i\})]^2 + \Gamma^2}, \tag{17}$$

and Γ represents the homogeneous (temperature) broadening.

III. SIMULATION RESULTS AND DISCUSSION

Next we implement the procedure described above to model the averaged intensity of the optical transitions for ensembles of the triple concentric GaAs/Al_xGa_{1-x}As nano-rings. By adjusting the model of Eq. (5), we fit the experimental data[20] and choose a basic geometrical shape of the rings (known from the experiment) as follows: $R_1 = 40$, $R_2 = 70$, and $R_3 = 105$ nm; $h_1 = 7$, $h_2 = 4$, and $h_3 = 3$ nm; $\gamma_{o1} = 30$, $\gamma_{o2} = 10$, and $\gamma_{o3} = 10$ nm; $\gamma_{i1} = 12$, $\gamma_{i2} = 22$, and $\gamma_{i3} = 5$ nm; and $h_{m3} = 1.95$ nm. The slope of the potential change at the boundaries of the ring is chosen as $a = 0.5$ nm. As an example, in Fig. 2 we show the radial profiles of the rings when only the inner height h_1 is varying. For GaAs/$Al_{0.3}Ga_{0.7}$As rings, we use realistic semiconductor material parameters known from the literature[19,26–28] and adjusted according to the composition and geometry.[20]

According to Ref. 20 and our calculation experience for the triple nano-rings, the ground-state wave functions of electrons and holes are localized in the inner ring. In addition, the excitonic-energy deviations are much more sensitive to the local height profile variations than to the radial deviations. For instance, the excitonic energy varies within the range of $\Delta E_{\text{ex}} \sim 0.9$ meV when the inner radius is changing within the range $\Delta R_1 \sim 5$ nm. At the same time, $\Delta E_{\text{ex}} \sim 3.5$ meV for $\Delta h_1 \sim 0.5$ nm. This suggests that the dispersion of the excitonic energy in the ring ensemble is in general determined by the variation of the inner height profile (the shape of the inner peak in Fig. 2). Therefore, in this paper we consider in detail only the variation of the local inner peak profile. We stress that, even if only the inner height h_1 varies, the parameters h_{m1} and h_{m2} have to be adjusted also to keep the overall radial height profile under control. For instance, for $h_1 = 7$ nm, we should take $h_{m1} = 6.75$ nm and $h_{m2} = 2.95$ nm.

The excitonic-transition energies for different values of h_1 are obtained numerically from solutions of the three-dimensional eigenvalue problem [Eq. (11)],[25] Poisson equation [(Eq. (14)], and Eq. (15) using the COMSOL Multiphysics package.[29] We fit the results of those simulations (Fig. 3) to the

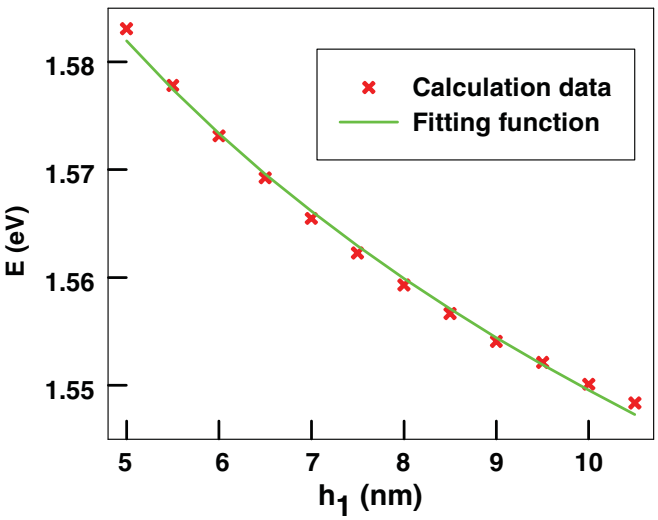

FIG. 3. (Color online) Excitonic-transition energies of triple GaAs/AlGaAs concentric nano-rings as a function of the inner height.

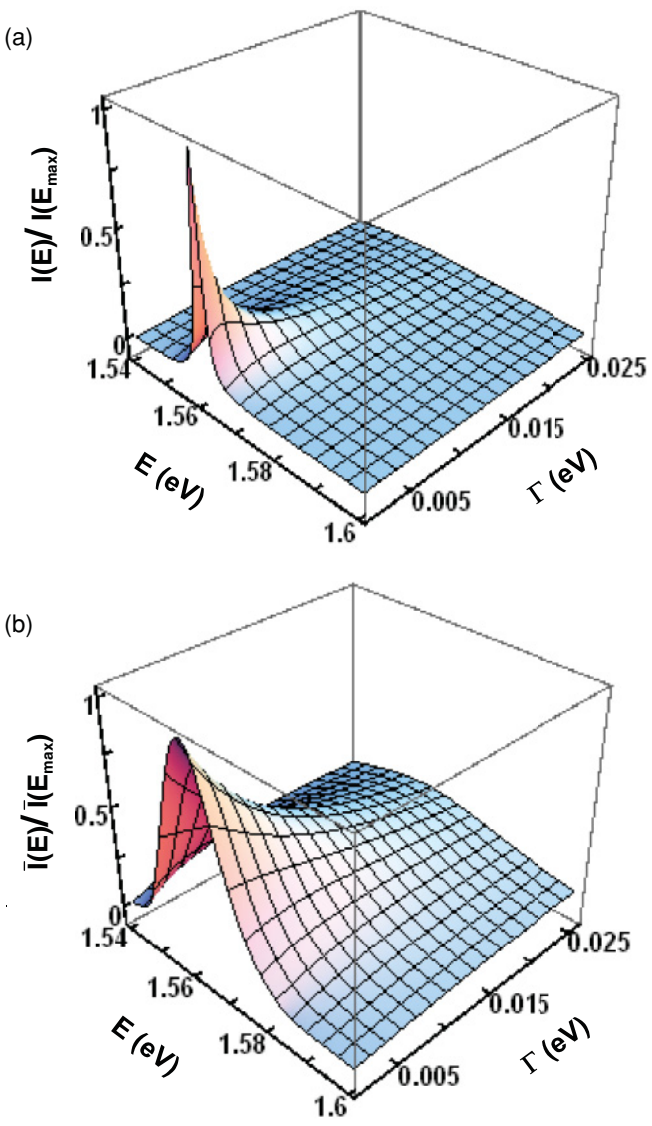

FIG. 4. (Color online) Normalized intensity of the excitonic optical transitions as a function of the transition energy and Γ: (a) an individual ring with the inner height $h_1 = 7.9$ nm and (b) ring ensemble with $h_1^0 = 7.9$ nm, $\Delta h_1 = 1.2$ nm. $E_{\max}$ is the position of the intensity maximum.

excitonic energy as a function of the inner height (h_1) using the following guess:

$$E_{\text{ex}}(h_1) = \frac{b}{(h_1)^c}. \tag{18}$$

According to our experience, the best fit can be achieved when $b = 1.66$ and $c = 0.03$ (in appropriate SI units). Substituting $E_{\text{ex}}(h_1)$ from Eq. (18) to Eq. (16), we are able now to simulate the inhomogeneous broadening of the excitonic emission peak for the dispersive ensembles of triple concentric nano-rings.

First, in Fig. 4(a) we present the normalized intensity of the excitonic optical transitions of an individual triple concentric nano-ring with the inner height $h_1 = 7.9$ nm. The intensity demonstrates a very sharp symmetrical peak when Γ is small (low temperature). The peak reaches the maximum at $E_{\text{ex}}^0 \approx 1.5602$ eV, which is in good agreement with the experimental data from Ref. 20. Clearly, for the individual ring, the width of the excitonic peak is governed by the homogeneous broadening only. The peak becomes wider and disappears very rapidly (but it still remains symmetrical) when Γ (temperature) increases. In contrast, the experimental data from Ref. 20 reveal the wide asymmetrical peak even at low temperatures ($T = 14$ K). Wide asymmetrical peaks can be explained only by the inhomogeneous broadening,[1,4] which is attributed to the geometry dispersion in the ring ensembles. To demonstrate this, we consider now the intensity of the excitonic optical transitions for the ensemble of the rings with the inner height variations. In Fig. 4(b) we present the normalized averaged intensity of the excitonic optical transitions for the ensemble of the rings with the mean value of the inner height $h_1^0 = 7.9$ nm and standard deviation $\Delta h_1 = 1.2$ nm. Clearly, the inhomogeneous broadening is predominant at low temperatures and, thus, makes the peak wide and asymmetrical. We also can conclude that, at relatively high temperatures, both the homogeneous and inhomogeneous broadenings equivalently contribute.

In Fig. 5(a) we show the normalized intensity of the excitonic optical transitions when the standard deviation Δh_1 ($h_1^0 = 7.9$ nm) is varying and $\Gamma = 1.2$ meV (which

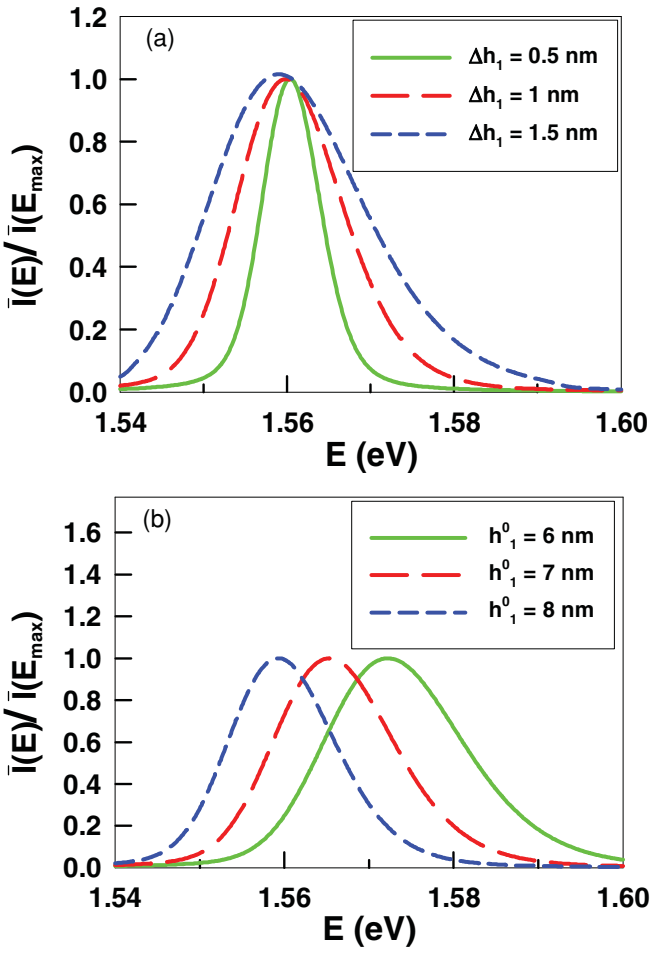

FIG. 5. (Color online) Normalized averaged intensity of the optical transitions of the ring ensemble as a function of the transition energy (Γ = 1.2 meV): (a) for different standard deviations of inner height and (b) for different inner heights ($\Delta h_1 = 1$ nm).

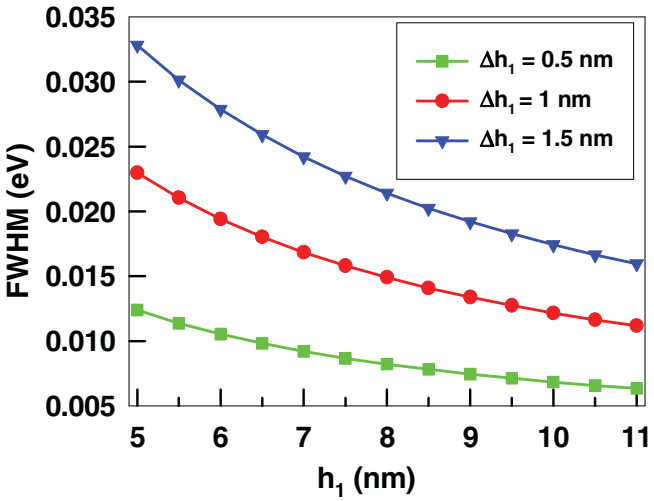

FIG. 6. (Color online) Full width at half maximum (FWHM) of the averaged intensity of the optical transitions of the ring ensemble as a function of the inner height for different standard deviations.

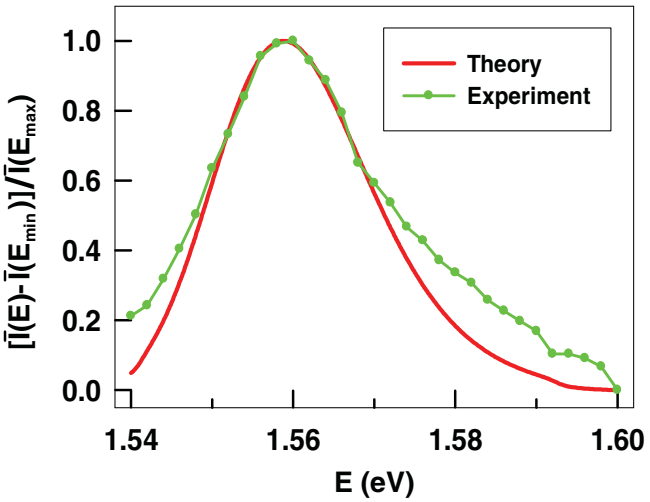

FIG. 7. (Color online) Normalized averaged intensity of the optical transitions of the ring ensemble as a function of the energy ($\Gamma = 1.2$ meV). $E_{\min}$ and $E_{\max}$ are the positions of the intensities' minimum and maximum.

corresponds to $T = 14$ K). Clearly, the asymmetry of the peak is growing with the standard deviation increasing. From Fig. 5(b) we also can conclude that when the mean value of the inner height (h_1^0) increases (Δh_1 is fixed to be 1 nm), the inhomogeneous broadening increases as well. In general, the increase of the relative standard deviation ($\Delta h_1/h_1^0$) enhances the inhomogeneous broadening of the excitonic peak. At the same time, the full width of the peak saturates for the relatively large inner heights (see Fig. 6).

Finally, to compare our results with experimental data from Ref. 20, in Fig. 7 we show the energy dependence of the normalized averaged intensity of the optical transitions of the ring ensemble with the mean value of the inner height $h_1^0 = 7.9$ nm and standard deviation $\Delta h_1 = 1.6$ nm at the low temperature ($T = 14$ K). Clearly, the peak that is located near the central transition energy of 1.5602 eV is wide, asymmetrical, and in very good agreement with the experiment. Within the low-temperature range, the homogeneous broadening plays a minor role and the inhomogeneous broadening dominates in the peak's full width.

IV. CONCLUSION

In conclusion, using our approach, we proposed a method to model the averaged intensity of the excitonic optical transitions for dispersive ensembles of semiconductor nano-objects of arbitrary geometrical shapes and material compositions. We demonstrated the method efficiency for the objects with a very sophisticated shape: triple concentric nano-rings. Our simulation results have explained the appearance and properties of the wide asymmetrical excitonic peaks in the photoluminescence spectra of the ring ensembles known from the experiment. The broadening is preferably caused by dispersion of the radial height profile (geometrical shape) of the rings in the ensembles (more specifically, the inner height). The calculated position of the excitonic peak in the optical spectrum is in good agreement with the experimental observations as well. The importance of homogeneous and inhomogeneous broadening at different temperature was analyzed.

We stress that, using our approach, we are able to clarify the important question of which geometrical and material parameter dispersions are crucial for the inhomogeneous broadening of optical spectra of ensembles of semiconductor nano-objects. The approach can be potentially useful for the realistic modeling of the inhomogeneous broadening of the excitonic peaks for dispersive ensembles of semiconductor nano-objects with arbitrary shape.

ACKNOWLEDGMENTS

This work is supported by the National Science Council of the Republic of China under Contracts No. NSC 97-2112-M-009-012-MY3, No. NSC 97-2120-M-009-004, and No. NSC 98-2918-I-009-001, and by the Ministry of Education of Taiwan under Contract No. MOEATU 95W803.

*minhthule1981@gmail.com

[1] V. I. Belyavskiĭ and S. V. Shevtsov, Semiconductors **36**, 821 (2002).
[2] D. L. Ferreira and J. L. A. Alves, Nanotechnology **15**, 975 (2004).
[3] V. Kumar and D. Biswas, J. Appl. Phys. **102**, 084305 (2007).
[4] V. V. Nikolaev and N. S. Averkiev, Appl. Phys. Lett. **95**, 263107 (2009).
[5] L. M. Thu and O. Voskoboynikov, AIP Conf. Proc. **1233**, 952 (2010).
[6] L. M. Thu and O. Voskoboynikov, Phys. Procedia **3**, 1133 (2010).
[7] A. Lorke, R. J. Luyken, A. O. Govorov, J. P. Kotthaus, J. M. Garcia, and P. M. Petroff, Phys. Rev. Lett. **84**, 2223 (2000).
[8] B. C. Lee, O. Voskoboynikov, and C. P. Lee, Physica E **24**, 87 (2004).

[9]Y. Aharonov and D. Bohm, Phys. Rev. **115**, 485 (1959).
[10]N. A. J. M. Kleemans, I. M. A. Bominaar-Silkens, V. M. Fomin, V. N. Gladilin, D. Granados, A. G. Taboada, J. M. García, P. Offermans, U. Zeitler, P. C. M. Christianen, J. C. Maan, J. T. Devreese, and P. M. Koenraad, Phys. Rev. Lett. **99**, 146808 (2007).
[11]P. Offermans, P. M. Koenraad, J. H. Wolter, D. Granados, J. M. García, V. M. Fomin, V. N. Gladilin, and J. T. Devreese, Appl. Phys. Lett. **87**, 131902 (2005).
[12]V. M. Fomin, V. N. Gladilin, S. N. Klimin, J. T. Devreese, N. A. J. M. Kleemans, and P. M. Koenraad, Phys. Rev. B **76**, 235320 (2007).
[13]V. M. Fomin, V. N. Gladilin, J. T. Devreese, N. A. J. M. Kleemans, and P. M. Koenraad, Phys. Rev. B **77**, 205326 (2008).
[14]N. A. J. M. Kleemans, J. H. Blokland, A. G. Taboada, H. C. M. van Genuchten, M. Bozkurt, V. M. Fomin, V. N. Gladilin, D. Granados, J. M. García, P. C. M. Christianen, J. C. Maan, J. T. Devreese, and P. M. Koenraad, Phys. Rev. B **80**, 155318 (2009).
[15]O. Voskoboynikov, Yiming Li, Hsiao-Mei Lu, Cheng-Feng Shih, and C. P. Lee, Phys. Rev. B **66**, 155306 (2002).
[16]J. I. Climente, J. Planelles, and W. Jaskólski, Phys. Rev. B **68**, 075307 (2003).
[17]T. C. Lin, C. H. Lin, H. S. Ling, Y. J. Fu, W. H. Chang, S. D. Lin, and C. P. Lee, Phys. Rev. B **80**, 081304(R) (2009).
[18]T. Mano, T. Kuroda, S. Sanguinetti, T. Ochiai, T. Tateno, J. Kim, T. Noda, M. Kawabe, K. Sakoda, G. Kido, and N. Koguchi, Nano Lett. **5**, 425 (2005).
[19]T. Kuroda, T. Mano, T. Ochiai, S. Sanguinetti, K. Sakoda, G. Kido, and N. Koguchi, Phys. Rev. B **72**, 205301 (2005).
[20]C. Somaschini, S. Bietti, N. Koguchi, and S. Sanguinetti, Nano Lett. **9**, 3419 (2009).
[21]G. Bastard, *Wave Mechanics Applied to Semiconductor Heterostructures* (Les Edition de Physique, Les Ulis, France, 1990).
[22]B. Szafran, S. Bednarek, and J. Adamowski, Phys. Rev. B **64**, 125301 (2001).
[23]D. Chaney, M. Roy, and P. Maksym, in *Quantum Dots: Fundamentals, Applications, and Frontiers*, edited by B. A. Joyce, P. C. Kelires, A. G. Naumovets, and D. D. Vvedensky (Springer, Dordrecht, The Netherlands, 2005), pp. 239.
[24]D. Schooss, A. Mews, A. Eychmüller, and H. Weller, Phys. Rev. B **49**, 17072 (1994).
[25]L. M. Thu and O. Voskoboynikov, Phys. Rev. B **80**, 155442 (2009).
[26]M. Yamagiwa, N. Sumita, F. Minami, and N. Koguchi, J. Lumin. **108**, 379 (2004).
[27]Sadao Adachi, J. Appl. Phys. **58**, R1 (1985).
[28]I. Vurgaftman, J. R. Meyer, and L. R. Ram-Mohan, J. Appl. Phys. **89**, 5815 (2001).
[29][www.comsol.com].